Materials Science & Engineering A 591 (2014) 54–58

Contents lists available at ScienceDirect

Materials Science & Engineering A

journal homepage: www.elsevier.com/locate/msea

Bulk multimodal-grained irons with large plasticity fabricated by spark plasma sintering

C. Yang [a,*], T. Wei [a], Y.P. Yao [a], Y.H. Li [a], S.G. Qu [a], L.C. Zhang [b]

[a] National Engineering Research Center of Near-net-shape Forming for Metallic Materials, South China University of Technology, Guangzhou 510640, People's Republic of China

[b] School of Engineering, Edith Cowan University, 270 Joondalup Drive, Joondalup, Perth WA 6027, Australia

ARTICLE INFO

Article history:
Received 26 August 2013
Received in revised form
19 October 2013
Accepted 22 October 2013
Available online 31 October 2013

Keywords:
Iron
Structural materials
Multimodal-grained structure
Spark plasma sintering
Mechanical properties

ABSTRACT

We report on the formation of a new bulk multimodal-grained (MGed) iron with a large true strain of 58% and high strength of 955 MPa by spark plasma sintering. The new MGed structure contains fine-grained α-Fe matrix and ultrafine-grained equiaxed and acicular α-Fe enhancing phases. The large plastic strain can be attributed to the increased dislocation motion and improved shear deformation ability resulted from such MGed structure containing three different α-Fe morphologies.

1. Introduction

Iron and its alloys are characterized by low cost, excellent mechanical properties and large-scale production, and have been the most widely used structural materials. However, there is still a great demand for improving their mechanical properties. Using an appropriate method to fabricate bulk irons with new structure and good combined mechanical properties has become an important research subject. As we all know, gain refinement is one of the most methods to improve strength and plasticity. According to Hall–Patch relation, the strength of a material can be increased gradually by decreasing coarse grain to fine grain (FG), ultrafine grain (UFG) and nanograin (NG) range. For example, UFGed irons with 150–300 nm [1] and 200–400 nm [2] in grain size processed by equal channel angular extrusion (ECAE) exhibit low yield strengths of about 600 and 700 MPa and large true strains of 20% and 30% under compression load, respectively. However, it has been reported that when grain size decreases to UFG or NG range the strength of a material is still high but the plasticity is severely degraded. Wang et al. [3] reported that UFGed titanium of ~260 nm prepared by ECAE exhibits a compression fracture strength of 1050 MPa, about 450 MPa higher than that of coarse-grained counterpart, but a lower fracture strain of 38% under the condition of true stress–strain. Jia et al. [4] showed that NG iron of 80 nm fabricated by hot press (HP) at 683 K displays a high compression fracture strength of more than 2500 MPa but a very low total strain of 5%, compared with a compression strength of about 1660 MPa and total strain of ~12% for HPed UFGed iron of 268 nm. Recently, it has been reported that the combined mechanical properties of materials can be improved by obtaining a bimodal-grained microstructure due to the occurrence of recrystallization. This is confirmed in the cases of Cu [5], Ti [6], Al [7], Ni [8], Fe [9], Fe–C [10]. Especially, Srinivasarao et al. [9] achieved a bulk bimodal-grained iron consisting of average FG of 2.5 μm and NG of 85 nm by spark plasma sintering (SPS) using step sintering method at 993 K, exhibiting a compressive yield and fracture strength of 1602 MPa and 2249 MPa, and a true strain of 40%.

However, the above step sintering technique used to control recrystallization process is complex and hard to obtain a certain proportion of FGed structure [5–10]. Besides, almost all aforementioned bulk irons were fabricated at relative low sintering temperature below its α→γ transformation temperature (1185 K), which is adverse for densification. Moreover, it can be expected that a materials with a bimodal-grained microstructure of FG and UFG, or multimodal-grained (MGed) one of FG and UFG in different morphologies, may possess larger plasticity and moderate fracture strength compared to a bimodal-grained one of FG and NG. It is well accepted that when sintering temperature is above α→γ transformation temperature, obtained bulk iron would undergo two phase transformations of α→γ and subsequent γ→α

* Corresponding author. Tel.: +86 20 87110099; fax: +86 20 87112111.
E-mail address: cyang@scut.edu.cn (C. Yang).

0921-5093/$ - see front matter © 2013 Elsevier B.V. All rights reserved.
http://dx.doi.org/10.1016/j.msea.2013.10.076

by nucleation and growth of crystals during whole sintering process. The special phase transformation is helpful for fabricating new metallic materials with high strength and plasticity. This has been proved by ultrahigh compressive specific strength and distinct ductility in FGed or UFGed Ti–O-based composites with hcp Ti_3O and hcp Ti phases [11]. Therefore, it is quite necessary to further investigate the microstructures and mechanical properties of bulk irons fabricated *above* its $\alpha \rightarrow \gamma$ transformation temperature by powder metallurgy.

In the present work, we report on the formation of a new bulk MGed iron containing a FGed α-Fe matrix and UFGed equiaxed and acicular α-Fe enhancing phases fabricated by SPS of ball-milled NG iron powder above its $\alpha \rightarrow \gamma$ transformation temperature. The as-fabricated bulk MGed iron exhibits large plasticity with a true strain of 58% as well as high strength of 955 MPa. The results obtained can provide insight into fabrication of new structure in metallic materials with excellent properties by phase transformation design.

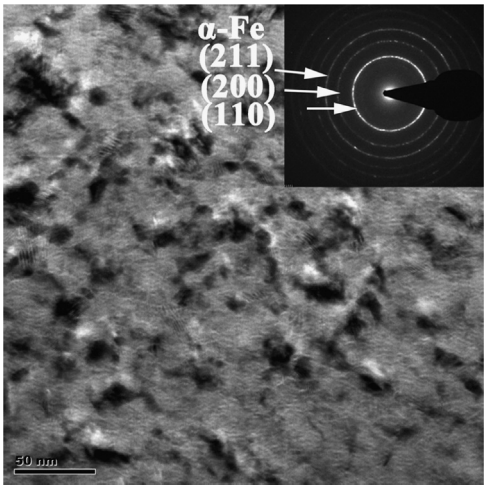

Fig. 1. TEM image and corresponding SAED pattern of the 75 h-milled iron powder.

2. Experimental procedure

NG iron powder was prepared by ball milling commercially pure iron powder of 99.5 wt% purity and 38 μm particle size in a QM-2SP20 high-energy planetary ball milling. Stainless steel balls of 15, 10, and 6 mm (1:3:1) were used with a ball-to-powder weight ratio of 10:1. The vial and the lid were sealed using an O-ring with a circular cross section. High-energy ball milling was performed for 75 h at 4.3 s^{-1} under a purified argon gas atmosphere (99.999%, 0.5 MPa), with an intermediate halt for 2 h after every 10 h milling to reduce the temperature rise. The as-milled iron powder was packed in a graphite die with an inner diameter of 10 mm and was sintered under argon atmosphere at a sintering pressure of 50 MPa by a Dr. Sintering SPS-825 system. The sintering of NG iron powder was done by heating at 373 K for 4 min, following by heating at 1253 K for 9 min (97 K/min) and holding for different times. The sintered samples fabricated had a cylindrical shape with a dimension of $\phi 10 \times 12$ mm.

The density with an uncertainty of 10^{-3} g for the as-sintered bulk samples was measured by the Archimedes' principle using water. The phase constituents and microstructures of the as-milled powders and the as-sintered and as-deformed bulk samples were examined by X-ray diffraction (XRD) with Cu K_α radiation, scanning electron microscopy (SEM) and transmission electron microscopy (TEM), respectively. To investigate fracture mechanism of the as-sintered bulk samples, nanoindentation experiments were conducted using a TriboIndenter® to determine hardness of different phase regions. The compressive mechanical properties of the as-sintered bulk samples were studied by uniaxial compression using a MTS TestStar 810 testing system at a strain rate of 5×10^{-4} s^{-1}. The test specimens with a dimension of $\phi 3 \times 6$ mm were used. Besides, the gas contamination content of O was determined by TC600 Nitrogen/Oxygen Determinator (LECO Co., US) with an uncertainty of 0.025 ppm.

3. Results and discussion

Fig. 1 shows TEM bright field image and corresponding selected area electron diffraction (SAED) pattern obtained from the iron powder after 75 h milling. It is found that the microstructure of the 75 h-milled iron powder is composed of randomly oriented NG α-Fe. Its average grain size and corresponding microstrain determined using the Scherrer formula [12,13] are approximately 12 nm and 0.16%, respectively. The oxygen content is 0.7 wt% according to the measurement of nitrogen/oxygen determinator.

Fig. 2(a) displays XRD patterns of the initial and as-milled powder and the as-sintered bulk irons. It can be clearly seen that after 75 h milling the intensity of NG α-Fe diffraction peaks decrease and the width increase, indicating that grain refinement takes place during the ball milling process. After sintering at 1253 K by SPS of the 75 h-milled iron powder, the intensities of α-Fe diffraction peaks in all bulk samples increase largely. This is attributed to grain growth and release of microstrain occurred during the SPS process. It is worthwhile noting that the XRD patterns indicate that the as-sintered bulk irons only consist of bcc α-Fe phase. Meanwhile, the location of α-Fe diffraction peaks has no significant shift under different holding times. When holding time varies between 0 min and 15 min, the lattice parameters of the bcc α-Fe phases are within 3.2170 ± 0.0052 Å.

Fig. 2(b)–(d) presents SEM micrographs of the as-sintered bulk irons by heating to 1253 K at 97 K/min and holding for different times. Compared with an UFGed α-Fe structure processed by ECAP [2] or HP [4] and a bimodal-grained structure of FGed and NG α-Fe fabricated by SPS [9], the microstructures of the as-sintered bulk irons are characterized by α-Fe matrix phase, the surrounded equiaxed α-Fe phase and acicular α-Fe phase, which are three different morphologies of α-Fe phase (Table 1). This is quite interesting and has never been reported so far. The formation of α-Fe matrix phase can be attributed to the fact that when sintering temperature is higher than $\alpha \rightarrow \gamma$ transformation temperature, α-Fe will partially transform into γ-Fe. Subsequently, when sintering temperature is lower than its $\alpha \rightarrow \gamma$ transformation temperature in cooling process, nucleation and growth of $\gamma \rightarrow \alpha$ occurs and finally α-Fe matrix forms when cooling to room temperature. The formation of the equiaxed α-Fe phase is the result of the incomplete $\alpha \rightarrow \gamma$ transformation during the SPS process and the residual NG α-Fe is preserved and grows in equiaxed shapes distributed along phase boundaries of α-Fe matrix when cooling to room temperature. The formation of the acicular α-Fe phase may result from that α-Fe phase nucleates heterogeneously at oxide particles (formed iron oxides induced by inevitably introduced oxygen and the oxygen contents of the as-sintered bulk iron is about 0.9%) and grows within original α-Fe matrix. This has been proved by formation of acicular α-Fe phase at oxide particles in low carbon steels under thermal treatment condition [14,15]. Besides, the process of the $\alpha \rightarrow \gamma$ transition progresses fuller with the extended holding time. This leads to a bigger volume fraction of α-Fe matrix phase and a smaller volume fraction of the equiaxed α-Fe phase (Fig. 2b–d). Meanwhile, the acicular α-Fe phase grows quickly and its length becomes longer as the holding time extends (Fig. 2b–d). Further TEM examinations as shown in Fig. 4 prove that the three